DESERT

DESERT
Online at http://jdesert.ut.ac.ir

DESERT 14 (2009) 185-196

Long Lead Flood Simulation Using Downscaled GCM Data in Arid and Semi-arid Regions: A Case Study

M. Karamouz[a*], M. Fallahi[b], S. Nazif[c], A. Ahmadi[c]

[a] *Professor, School of Civil Engineering, University of Tehran, Tehran, Iran*
[b] *M.Sc., School of Civil Engineering, Amirkabir University of Technology, Tehran, Iran*
[c] *Ph.D. Candidate, School of Civil Engineering, University of Tehran, Tehran, Iran*

Received: 29 December 2008; Received in revised form: 14 February 2009; Accepted: 3 May 2009

Abstract

Flood is one of the most calamitous natural disasters that causes extensive property and life damages across the world. It however, could be a blessing due to its special natural water resources recharging value. By simulating the magnitude of probable floods considering the anthropogenic and natural effects and implementing contingency plans, their damages could be reduced. In this paper, the General Circulation Model (GCM) climate change scenarios are employed to simulate future floods. The GCM scenarios include simulation of climatic signals of the future considering green house gas emission forces. In this study a statistical downscaling model (SDSM) has been applied for rainfall downscaling to provide regional results from GCM outputs. Then, a rainfall-runoff model called HEC-HMS has been employed to estimate runoff in the region. The maximum simulated rainfall for each year that is of high enough potential to cause flood, is introduced into the rainfall-runoff model to simulate the plausible hydrograph of the flood. The proposed procedure is applied to the Kajoo River basin in South Baloochestan region, south-east of Iran.

Keywords: Downscaling; Flood simulation; Rainfall-Runoff model; GCM

1. Introuduction

Flood is a natural disaster which can cause extensive damages and loss of life, however, it sometimes is considered as life saving due to water scarcity in arid and semi-arid regions. In some such regions as the southeastern Iran, the occurrence of a considerable downfall of rain in a short lapse of time often results in flash floods.

Many parts of the world have experienced changes in global water cycle such as the magnitude and timing of runoff, the frequency and intensity of floods and droughts, rainfall patterns, extreme weather events, and water availability both quantity and qualitywise (Jiang et al., 2007). Climate change has been realized as an effective factor on these changes in recent years. Studies show that climate change has significant impacts on the medium to long-term planning of water resources as well as on flood characteristics (IPCC, 1999).

Over the last decade, two main strategies have evolved in assessing the hydrological effects of climate change. The first is to identify past hydroclimatic variations over appropriate timescales by examining change in rainfall and runoff. This strategy is crucially dependent on the availability and quality of appropriate long-term records (Hisdal et al., 1995). The second strategy, which has been rapidly developed over the last decade, involves the development of climate change scenarios (based on the estimates of future trends in global population, economic and technological developments and the resulting behavior of climatic system) coupled with GCMs (General Circulation

[*] Corresponding author. Tel.: +98 21 88555854, Fax: +98 21 88701507.
E-mail address: karamouz@ut.ac.ir

Models) and then downscaling of outputs of rainfall and temperature at the regional or catchment scales. Rainfall-runoff models are applied to the downscaled hydro-meteorological variables to provide estimates of change in runoff under the specified climatic scenarios (Arnell, 1997; Reynard et al., 1998; Kilsby et al., 1998). It is not possible to make reliable predictions of regional hydrologic changes directly from climate models due to the coarse resolution of GCMs and the simplification of hydrologic cycle in climate models (Arora, 2001). A successful implementation of climate change scenarios is significantly dependent on better specified scenarios; increasingly accurate GCM outputs (especially for precipitation); improved procedures for downscaling to meso-size catchments; and precise calibration of selected rainfall-runoff models. As there is not enough historical data available in most of the cases, applying the second strategy for evaluation of climate change impacts would be more practical and beneficial.

In this paper, the second approach is employed to evaluate climate change effects on runoff for Kajoo River basin located in south-eastern Iran. The method has been applied for long-lead flood simulation, using downscaled rainfall data. The downscaled rainfall data are used as input into rainfall-runoff model, which has been calibrated as based on historical flood events for simulation of future flood hydrographs. In a next section a brief description of the structure of GCM and rainfall downscaling procedure has been given. This section is followed by introducing the study area and data resources. Then a description of structure of rainfall- runoff model and its calibration procedure is given. Finally a summary and conclusion under the topic of discussion and conclusionis presented.

2. Materials and methods

2.1. General Circulation Model (GCM)

General Circulation Models (GCMs) indicate that rising concentrations of greenhouse gases will have significant implications for climate at global and regional scales. GCMs describe the atmosphere at rectangular grids covering the earth with cubes of air above which currently are 2-5° grid in latitude and longitude, 6-15 vertical levels which are assumed as representatives of volume elements in the atmosphere as presented in Figure 1.

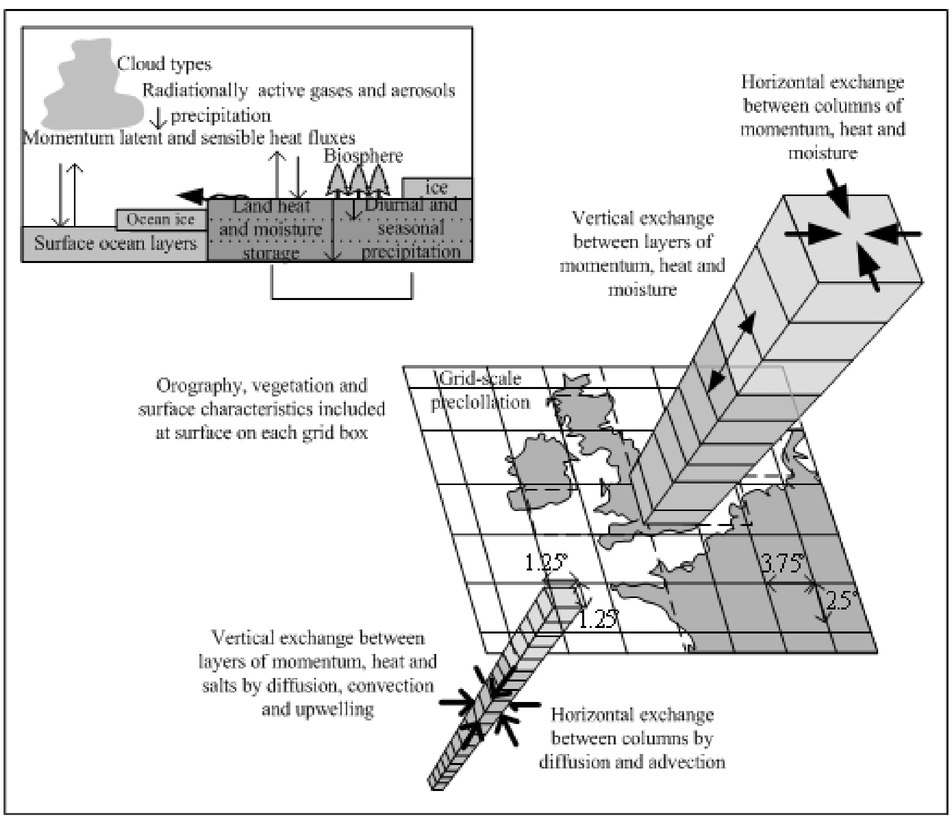

Fig. 1. A schematic discrete of atmosphere for utilizing GCMs (Wilby and Wilks, 2002)

These models solve a series of equations in the atmosphere describing movement of energy and momentum along with conservation of mass and water vapor as follows:

1- Momentum equation:

$$\frac{D\bar{v}}{Dt} = -2\bar{\Omega}\wedge\bar{v} - \left(\rho^{-1}\right)\nabla.p + \bar{g} + \bar{F} \qquad (1)$$

2- Mass conservation equation:

$$\frac{Dr}{Dt} = -\rho\left(\nabla.\bar{v}\right) + C - E$$

(2)

3- Energy conservation equation:

$$\frac{DI}{Dt} = -p\frac{d\rho^{-1}}{dt} + Q$$

(3)

4- Gas Law:

$$p = \rho RT \qquad (4)$$

Where $\frac{D}{Dt} = \frac{\partial}{\partial t} + \bar{v}.\nabla$, $\bar{v}$ is velocity relative to rotating earth, t is time, $\bar{\Omega}$ is angular velocity vector of the earth, ρ is the atmospheric density, g is apparent gravitational acceleration, $\bar{F}$ is force per unit mass, C and E are rate of creation and destruction of atmospheric constituents, I is internal energy per unit mass ($I=c_v.T$), Q is heating rate per unit mass, R is gas constant, T is temperature and c_v is specific heat of air at constant volume and p the atmospheric pressure. These equations are solved defined values of divergence terms at each grid point, and defined input and output for upper and lower surfaces of array is solved for each defined element of the atmosphere.

The climatic variables which are pressure dependent are analyzed on such iso-pressure heights as 500-hpa or 850-hpa heights. The air pressure varies with height from ground surface but its variations are terrain following (Figure 2).

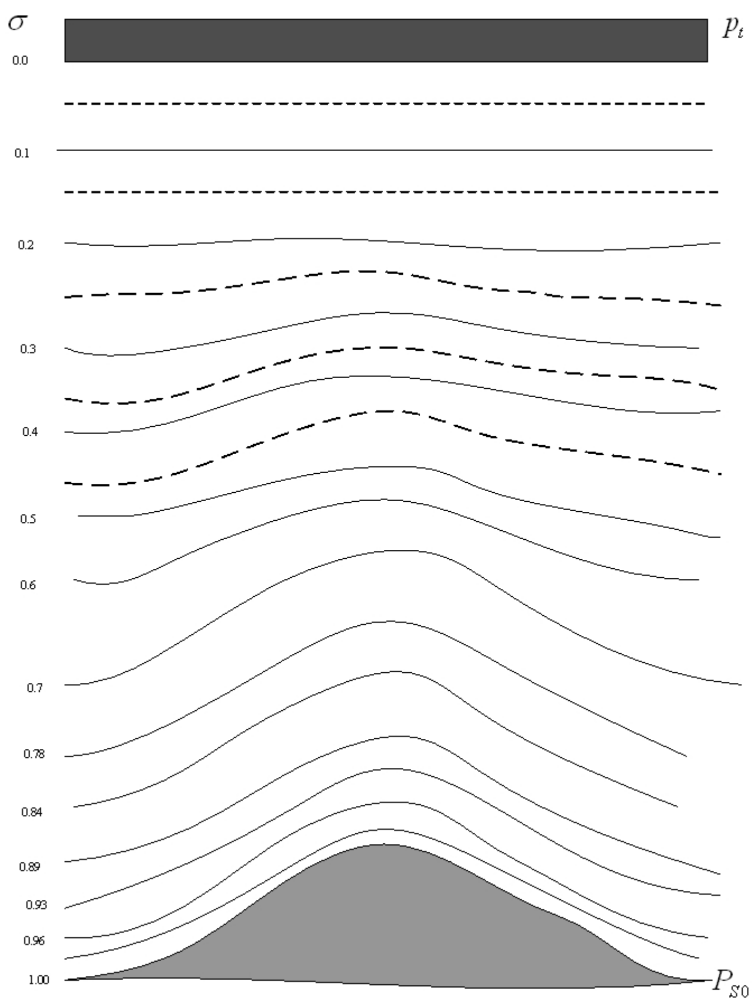

Fig. 2. Schematic representation of the vertical variation of pressure

By being elevated from ground surface, the iso-pressure lines get smoother and straight, or meaning that the lower grid levels follow the terrain while the upper surface is flat. A dimensionless quality σ is used to define the model levels:

$$\sigma = \frac{p_0 - p_t}{P_{S0} - p_t} \tag{5}$$

Where P_0 is the reference-state pressure, P_t is a specified constant top pressure, and P_{S0} is the reference-state surface pressure. It can be seen from Equation 5 and from Figure 2 that σ is zero at the model top while one at the model surface, each model level being defined by a value of σ. As GCMs are run at a low resolution, the results should be downscaled into watershed scale at individual stations (Department of the Environment, 1996). A brief description of the downscaling techniques is given in the next section.

2.2. Downscling techniques

The general theory, limitations and practice of downscaling, have been discussed in detail by Giorgi and Mearns, (1991); Wilby et al., (1998) and by Xu, (1999). Local-scale surface weather could be derived in two levels from regional-scale atmospheric predictor variables as illustrated in Figure 3. Firstly, Statistical Down Scaling (SDS) is analogous to the "Model Output Statistics" (MOS) and "perfect prog" approaches used for short-range numerical weather predict (Wilby and Wilks, 2002). Secondly, in a dynamical style of approach, Regional Climate Models (RCMs) are used to simulate sub-GCM grid scale climate features dynamically using time-varying atmospheric conditions supplied by a GCM bounding a specified domain. Both approaches will continue to play a significant role in the assessment of potential climate change impacts arising from future increases in greenhouse-gas concentrations.

2.2.1. Statistical Down Scaling Model (SDSM)

SDSM uses statistical downscaling methodology that enables the construction of climate change scenarios for individual sites at daily time-scales, using grid resolution GCM output. Statistical downscaling methods rely on empirical relationships between local scale predictants and regional scale predictor(s). The main advantage of this technique is the relative ease of application coupled with observable trans–scale relationships. The main weakness of regression–based methods is that the models often explain only a fraction of the observed climate variability (especially in precipitation series). Regression methods also assume validity of the model parameters under future climatic conditions, and are highly sensitive to the choice of predictor variables and to statistical transfer function. Furthermore, downscaling future extreme events using regression methods is problematic since these phenomena, by definition, tend to lie at the limits or beyond the range of the calibration data set (Wilby et al., 1998).

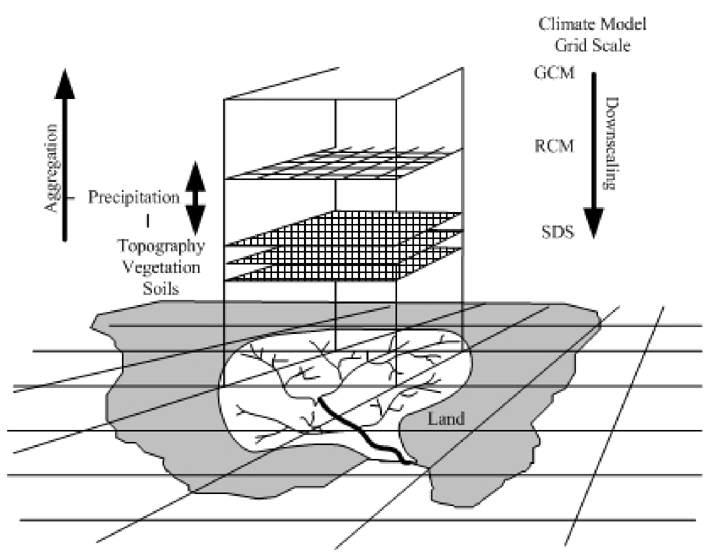

Fig. 3. A schematic illustration of downscaling levels (Wilby and Dawson, 2004)

During downscaling with the SDSM, a multiple linear regression model is developed between a few selected large-scale predictors and local scale predictants such as temperature and rainfall. The parameters of the regression equation are estimated using the efficient dual simplex algorithm. Large-scale relevant predictors such as weather pressure, temperature, velocity and humidity are selected using correlation analysis, partial correlation analysis and scatter plots, and also considering physical sensitivity between selected predictors and predictant for the region. Ideally, predictor variable candidates should be physically and conceptually sensible with respect to the predictant (rainfall) and accurately modeled by GCMs. In rainfall downscaling, it is also recommended that the selected predictors should contain variables describing such atmospheric circulations as thickness, stability and moisture content. In practice, the choice of predictor variables is constrained by data availability in GCM archives. Structure and operation of SDSM includes five distinct tasks as presented in Figure 4, and as follows: (1) preliminary screening of potential downscaling predictor variables; (2) assembly and calibration of SDSM(s); (3) synthesis of ensembles of current weather data using observed predictor variables; (4) generation of ensembles of future weather data using GCM-derived predictor variables; (5) diagnostic testing/analysis of observed data and climate change scenarios. In this model, the first step is to determine whether daily rainfall occurs or not. For this purpose ω_i, the indicator of state of rainfall either occurring or not on day i is calculated as follows:

$$\omega_i = \alpha_0 + \sum_{j=1}^{n} \alpha_j \hat{u}_i^{(j)} \tag{6}$$

Where $\hat{u}_i$ is the normalized predictor on day i and α_j the estimated regression coefficient. Precipitation in day *i* occurs if $\omega_i \leq r_i$, where r_i is a stochastic output from a linear random-number generator.

Value of rainfall in each rainy day is estimated in the second step using z-score as follows:

$$Z_i = \beta_0 + \sum_{j=1}^{n} \beta_j \hat{u}_i\,(j) + \varepsilon \tag{7}$$

where Z_i is the z-score for day *i*, β_j the estimated regression coefficients for each month, ε is a normally distributed stochastic error term, and

$$y_i = F^{-1}[\phi(Z_i)] \tag{8}$$

Where ϕ is the normal cumulative distribution function and *F* the empirical function of y_i, daily precipitations.

2.3. Study area

The study area is the Kajoo River sub-basin with an area of about 3659 km^2, located in Sistan- Baloochestan province, south-eastern Iran. Because of the limited carrying capacity of Kajoo River, yearly floods inflict severe damages to agricultural lands and to rural areas. Therefore, hydrograph simulation of probable future floods of the region is the first and most vital step in developing an appropriate scheme for contingency plans to face the floods. Twenty four year (1976–1999) data of daily rainfall of a meteorological station inside the basin namely Ghasre-Ghand, is taken for downscaling rainfall as predictant. Such observed large-scale NCEP (National Centre for Environmental Prediction) atmospheric variables as air pressure, humidity, velocity in different atmospheric levels for the same period (for 60-63.75E, 25-27.5N) have been used as rainfall predictors. The library of large-scale NCEP predictors is divided into the regions of: Europe, Africa and Middle East, Asia as well as 3 regions in America. The considered case study is placed in Asian division, located at 60-63.75 E longitude and 27.5-30 N latitude as illustrated in Figure 5 (The grid covering the earth in library of NCEP is 2.5 in latitude and 3.75 in longitude).

Weather generator is employed to downscale observed NCEP predictors, and to generate scenarios to downscale the considered scenarios for future climate variations. HadCM3 (Second Hadley Centre Coupled Ocean-Atmosphere GCM) scenario A data which is available from 2000 to 2099, is used to simulate the future rainfall under climate change effects. In these scenarios, the effect of greenhouse gas emissions on climate, and their subsequent effects on the future economic and social development are taken into consideration.

3. Results

3.1. Rainfall Downscaling

SDSM uses normal distributed data in downscaling procedure so, at first daily rainfall data has been transformed through the fourth root function to fit the normal probability distribution. The correlations between different combinations of available predictors and daily rainfall have been assessed to find the most appropriate set of predictors. It should be noted that correlations between winter rainfall and predictors have been considered because it is in this season that the more severe floods occur.

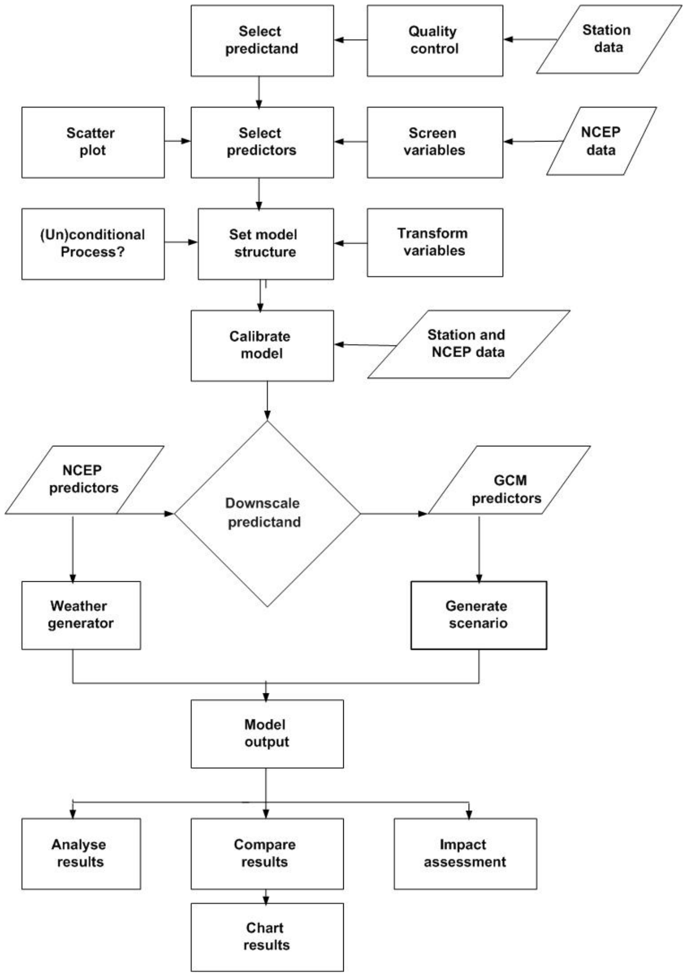

Fig. 4. SDSM climate scenario generation process (Wilby et al., 2002)

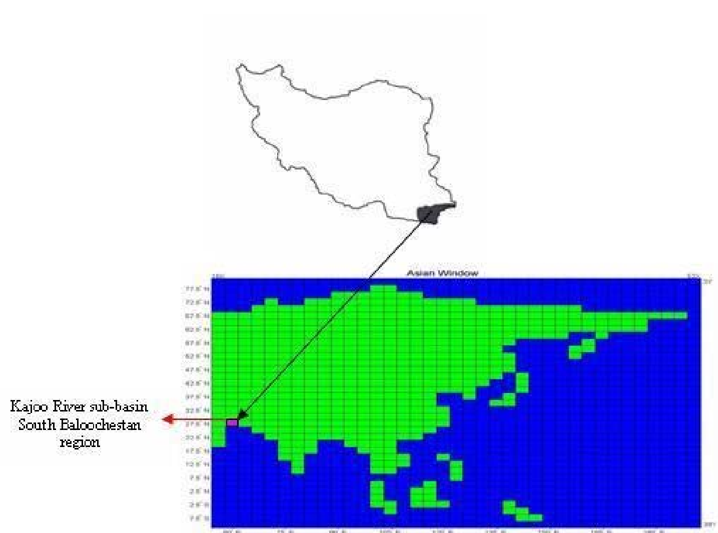

Fig. 5. Location of the Baloochestan province in the NCEP archive

P-value and correlation statistics between rainfall and predictors available in SDSM library have been used to select the more effective predictors in rainfall prediction. P-value helps to identify the extent of explanatory power for each predictor. P-values lower than 0.05 indicate that the result can be statistically significant but not assuredly of practical significance. On the other hand a high P-value would indicate that the predictor-predictant correlation is likely to be due to chance. The drawn scattered plots for visual inspection of predictor and predictant's relations are also employed to demonstrate the relationship between rainfall and the selected set of predictors. Finally the set of predictors has been selected for long lead rainfall simulation as based on maximum correlation with daily rainfall, presented in Table 1. Results show that the most effective signals are the relative humidity at 850 hPa height, near surface specific humidity as well as near surface relative humidity. Air humidity is the most effective factor on rainfall in the study region with all the selected predictors being related to humidity.

Table 1. The selected effective climate variables for long lead rainfall simulation in the Baloochestan area

Predictor	Correlation coefficient	Partial correlation coefficient	P value
Relative humidity at 850 hPa height	0.42	0.48	0.002
Near surface specific humidity	0.40	0.44	0.000
Near surface relative humidity	0.45	0.50	0.000

The model has been calibrated against rainfall data for years 1976-1990 and validated for the remaining available data (1991-1999). Monthly, seasonal and annual mean as well as standard deviation statistics in the calibration period have been shown in Table 2. As can be seen the statistics of the simulated and observed data are close to each other with their difference in all the considered time steps being always less than 10%. This shows the robust performance of the model which is a condition necessary for long lead rainfall simulation.

Through the above procedure, the weather generator was employed to downscale the observed (NCEP) predictors, and generate scenarios to downscale the GCM predictors representing the current climate. Figure 6 shows the compatibility of monthly mean rainfall totals under observed (NCEP) and HadCM3 (Second Hadley Centre Coupled Ocean-Atmosphere GCM) during the validation period. As can be seen in this figure the maximum differences occur in February, June and December. The observed against simulated total rainfall in the three winter months, December, January and February, are 89 and 85 respectively, resulting in about 5% error in long lead rainfall simulation. The simulated rainfall values from 1961 to 2099 (Fig. 7) are compared to evaluate the effect of climate change on annual rainfall. The mean value of rainfall in the period 2006 to 2099 will decrease for about 3% rather than the mean value of historical records (1961-2005). The severity of the rainfall events especially the peak values will decrease under climate change effects in the study region. The decrease of standard division by 12% in the future demonstrates this fact.

3.2. Rainfall-Runoff Model

In order to simulate runoff as based on rainfall, the hourly hyetograph of rainfall is developed using rainfall pattern suggested by NRCS (Natural Resource Conservation Service, 1986). For this purpose, the rainfall pattern of study area developed by Absaran Consulting Engineers (2005) has been compared with the three suggested SCS patterns for disaggregation of total rainfall. Finally, the central SCS pattern has been selected because of better coincidence with the observed rainfall pattern in the region. The selected pattern has monotonic and steady intensity during the rain, the same as the observed rainfall pattern in the study area.

HEC- HMS model developed by Hydrologic Engineering Center of U.S Army Corp of Engineers is used as the rainfall-runoff model in this study. Sub-basins of the study area have been characterized and modeled in HEC-HMS software using SCS method. The study area includes 12 sub-basins the physical characteristics of which and their placement in the study area are presented in Table 3 and in Figure 8, respectively. These sub basins are identified as based on the topographic characteristics of the study region. There exist three hydrometric (H1-H3) and three gage stations (R1-R3) in the study area as presented in Figure 8. The recorded data at these stations are employed for development of rainfall-runoff model.

Table 2. Summery statistics of observed and simulated data

Month	Mean	Max	Min	Variance	Summation
Summery statistics of observed data					
January	0.26	2.58	0.1	0.25	7.73
February	0.176	2.5	0.1	0.12	4.84
March	0.27	2.8	0.1	0.27	8.32
April	0.12	2.07	0.1	0.03	3.61
May	0.12	1.86	0.1	0.03	3.63
June	0.13	2.08	0.1	0.05	3.92
July	0.17	2.24	0.1	0.12	5.24
August	0.14	2.14	0.1	0.06	4.32
September	0.12	1.73	0.1	0.02	3.47
October	0.18	2.32	0.1	0.13	5.50
November	0.12	2.00	0.1	0.36	3.68
December	0.21	2.46	0.1	0.18	6.57
Winter	0.21	2.57	0.1	0-.19	17.22
Spring	0.17	2.80	0.1	0.11	15.57
Summer	0.15	2.25	0.1	0.78	13.48
Autumn	0.14	2.32	0.1	0.07	12.65
Annual	0.17	2.80	0.1	0.11	60.84
Summery statistics of simulated data					
January	0.27	2.5	0.1	0.29	8.5
February	0.32	2.69	0.1	0.36	8.9
March	0.2	2.67	0.1	0.19	6.3
April	0.17	2.47	0.1	0.11	4.9
May	0.12	2.14	0.1	0.05	3.8
June	0.11	1.86	0.1	0.01	3.2
July	0.19	2.74	0.1	0.17	5.89
August	0.18	2.51	0.1	0.14	5.68
September	0.13	1.73	0.1	0.04	3.49
October	0.13	1.86	0.1	0.04	3.91
November	0.12	2.19	0.1	0.027	3.46
December	0.19	2.43	0.1	0.14	5.73
Winter	0.25	2.68	0.1	0.26	21.56
Spring	0.16	2.67	0.1	0.12	15.03
Summer	0.16	2.73	0.1	0.11	14.74
Autumn	0.12	2.19	0.1	0.03	10.87
Annual	0.17	2.74	0.1	0.13	59.52

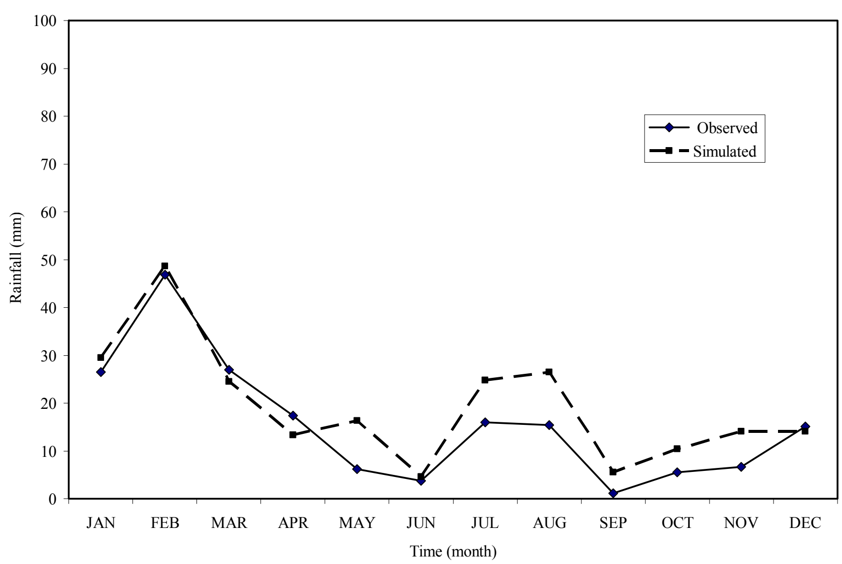

Fig. 6. Monthly mean rainfall totals at Baloochestan for the current climate downscaled using observed (NCEP) rainfall

(1991-1999) and GCM (HadCM3) predictors (1991-1999)

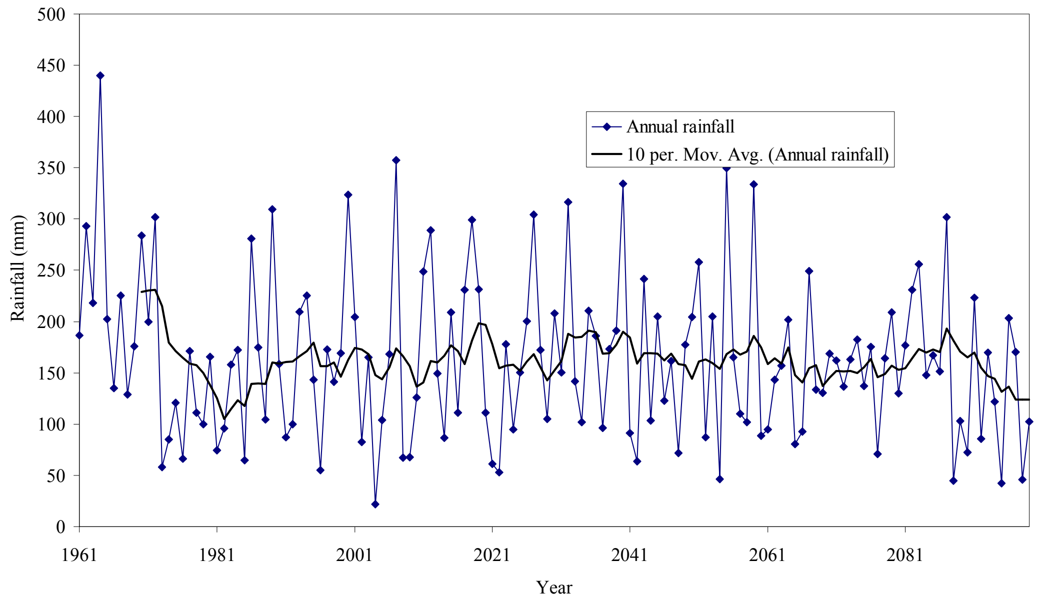

Fig. 7. The annual rainfall variations for the period of 1961-2005 (historical) and 2006-2099 (simulated)

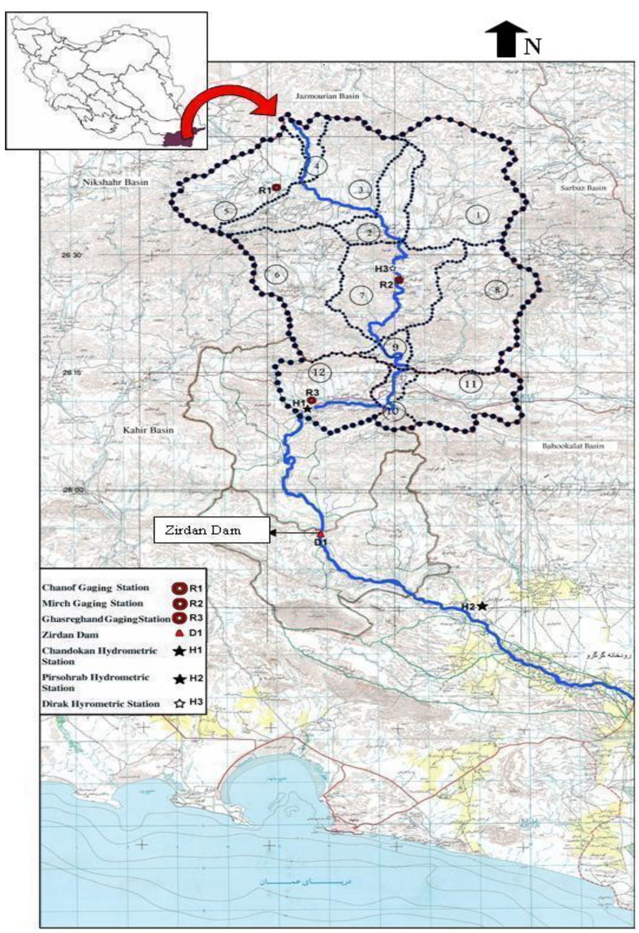

Fig. 8. Sub-basins of the study area

Table 3: The characteristic of sub-basins in the study area

Sub-basin	A (km^2)	L (km)	t_C (Kirpich)
1	535	28	3.48
2	175	10	1.01
3	422	21	2.34
4	66	13	1.56
5	317	38	1.49
6	450	39	4.26
7	395	39	5.12
8	506	32	3.46
9	50	13	1.61
10	73.3	13	1.75
11	255	25	3.18
12	295	18	1.9

For development of the rainfall-runoff model, first, the basin physiographic parameters including *CN*, time of concentration and the initial loss of rainfall are determined. Since different sub-basins have different *CN* values, the area-weighted of *CN*s is considered as the representative of soil condition in the entire basin. An average *CN* of 85 has been estimated for the basin in a moderate humidity (AMC-II) situation. The initial loss of rainfall has been considered as 3 mm according to site measurements. The time of concentration, t_c, is estimated using Kirpich method as follows:

$$t_c = 0.949\left(\frac{L^3}{H}\right)^{0.385} \tag{9}$$

Where *L* is the length of flow in the basin (km) and *H* the altitude difference between outlet and highest point of the basin.

A historical storm hyetograph occurred in January 1998 has been chosen for rainfall-runoff model calibration. The observed and simulated hyetographs of this storm have been shown in Figures 9 and 10. The schemes of the observed and predicted rainfall in the first day are different but during the next day the difference between the observed and predicted values decreases. There is about 15% difference between the predicted and observed recordings of rainfall during the thunderstorm days of January 28 and 29, 1998. The predicted values are overestimated and more conservative. The observed and simulated hydrographs of this storm have been shown in Figure 11 with R^2 equal to 96%. Although the observed hydrograph bears two distinct peaks with its major peak bearing about 50% error (the difference of observed and simulated values divided by the observed value), the volumes of observed and simulated flood hydrographs of 20% error are closer to each other. It can be concluded that the proposed methodology can effectively simulate the flood volume but further studies should be carried out to improve the temporal distribution of flood hydrograph.

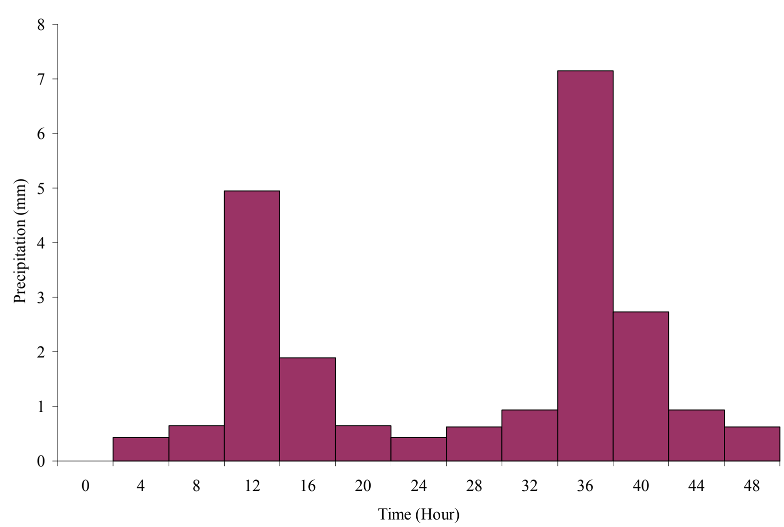

Fig. 9. The observed hyetograph of storm during 28-29 January 1998

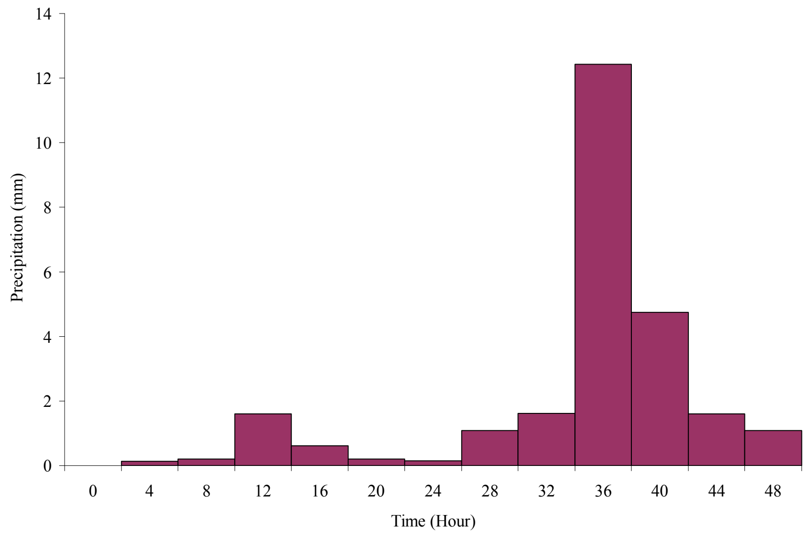

Fig. 10. The simulated hyetograph of storm during 28-29 January 1998

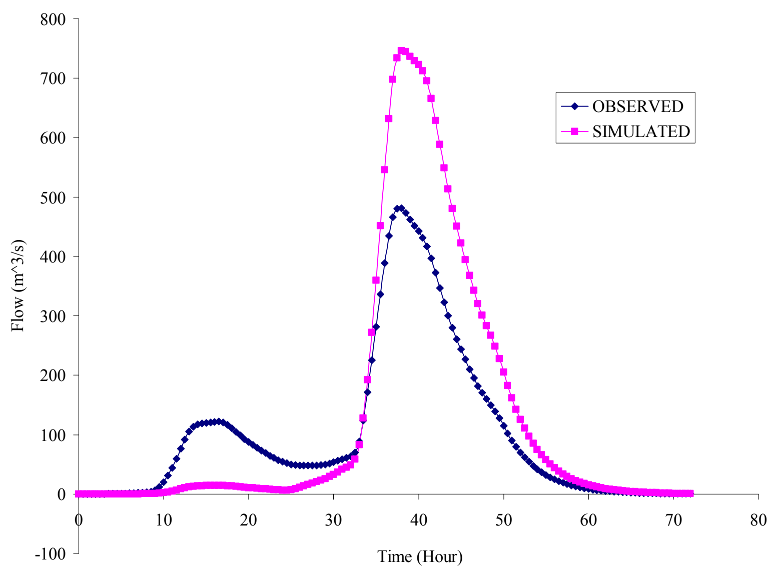

Fig. 11. A comparison of the simulated and observed hydrograph of storm occurred during 28-29 January 1998

4. Discussion and conclusion

Winter rainfall predicted through GCM scenarios have been downscaled using large scale NCEP signals and SDSM for South Baloochestan region in Iran. Different large scale predictors have been examined for a prediction of rainfall out of which surface specific humidity, near surface specific humidity, relative humidity at 850 hpa which were observed to be of the highest correlation with daily rainfall, were selected.

Through an analysis of the downscaled rainfall data for each year, the flood generating rainfall has been simulated in the HEC-HMS rainfall-runoff model to simulate flood hydrograph. The results show that the simulated hydrograph volume closely matches with the observed value. This combined model can be employed for flood simulation as an effective tool and it can help decision makers in planning for appropriate on-time emergency response strategies to reducethe extent of flood damages.

5. Acknowledgments

This study was carried out at the University of Tehran as part of a project entitled "Flood plain zoning downstream of Kajoo and Kariani river basins and the design of a flood warning system" sponsored by the Sistan and Baloochestan Water Authority.

Index

t: time
$\bar{v}$: velocity relative to rotating earth
$\bar{\Omega}$: angular velocity vector of the earth
ρ: atmospheric density,
g: apparent gravitational acceleration
$\bar{F}$: force per unit mass
C: rate of creation of atmospheric constituents
E: rate of destruction of atmospheric constituents
I: internal energy per unit mass ($I=c_v.T$)
Q: heating rate per unit mass
R: gas constant,
T: temperature
c_v: specific heat of air at constant volume
P: atmospheric pressure
$\hat{u}_i$: normalized predictor on day i
α_j: the estimated regression coefficient
r_i: a stochastic output from a linear random-number generator
Z_i: the z-score for day i
β_j: monthly estimated regression coefficients
ε: a normally distributed stochastic error term
ϕ: the normal cumulative distribution function
F: the empirical function of y_i
L: length of flow in the basin (km)
H:altitude difference between outlet and the highest point of the basin

References

Arnell, N.W., N. Reynard, R. King, C. Proudhomme and J. Branson, 1997. Effects of climate change on river flows and groundwater recharge: guidelines for resource assessment. Environment Agency Technical Report W82, Bristol.

Arora, V.K., 2001. Streamflow simulations for continental-scale river basins in a global atmospheric general circulation model. Advances in Water Resources 24, 775–791.

Burger, C.M., O. Kolditz, H.J. Fowler and S. Blenkinsop, 2007. "Future climate scenarios and rainfall-runoff modelling in the Upper Gallego catchment (Spain)", Elsevier, journal of Environmental Pollution.

Department of the Environment, 1996. Review of the potential effects of climate change in the United Kingdom. HMSO, London, PP. 247.

Giorgi, F. and L.O. Mearns, 1991. Approaches to the simulation of regional climate change. A review. Review of Geophysics 29, PP. 191-216.

Hisdal, H., J. Erup, K. Gudmundsson, T. Hiltunen, T. Jutman, N.B. Oversen and L. Roald, 1995. Historical runoff variations in the Nordic countries. Nordic Hydrological Programme, NHP Report 37, Nordic Hydrological Council, Oslo, Norway.

Ingram, J.J., D.L. Fread and L.W. Larson, 1998, "Improving Real Time Hydrological Service in the USA, PartI: Ensemble Generated Probabilistic Forecast", British Hydrological Society.

IPCC, 1999. Guidelines on the Use of Scenario data for Climate Impact and Adaptation Assessment. Version 1. Prepared by

Jiang, T., Z.W. Kundzewicz and B. Su, 2007. Changes in monthly precipitation and flood hazard in the Yangtze River Basin, China. International Journal of Climatology, DOI: 10.1002/joc.1635

Kilsby, C.G., P.S.P. Cowpertwait, P.E. O'Connell, and P.D. Jones, 1998. Predicting rainfall statistics in England and Wales using atmospheric circulation variables. International Journal of Climatology 18, 523-539.

Reynard, N.S., C. Proudhomme and S.M. Crooks, 1998. The potential impacts of climate change on the flood characteristics of a large catchment in the UK. Proc. of the Second International Conference on Climate and Water, 1, Espoo, Finland. PP. 320-332.

United States Department of Agriculture (USDA). Natural Resources Conservation Service (NRCS), 1986. Technical Release 55: Urban Hydrology for Small Watersheds, 2nd Edition. Washington, D.C.

Wilby, R.L., T.M.L. Wigley, D. Conway, P.D. Jones, B.C. Hewitson, J. Main and D.S. Wilks, 1998. Statistical downscaling of general circulation model output: a comparison of methods. Water Resources Research 34, PP. 2995-3008.

Wilby, R.L. and C.W. Dawson, 2004. Using SDSM Version 3.1 - A decision support tool for the assessment of regional climate change impacts.

Wilby, R.L. and D.S. Wilks, 2002. The weather generation game: a review of stochastic weather models. Progress in Physical Geography 23, 329-357.

Xu, C.Y., 1999. From GCMs to river flow: a review of downscaling methods and hydrologic modelling approaches. Progress in Physical Geography 23, PP. 229-249.